Optical and Quantum Electronics (2021) 53:296
https://doi.org/10.1007/s11082-021-02960-6

# Theoretical characterization of induced ferromagnetism, half-metallic behavior, electronic properties in new Ti-doped BaO

**Malika Hachemaoui[1] · Mohamed Meskine[1] · Allel Mokaddem[2,3] · Bendouma Doumi[1,2] · Yesim Mogulkoc[4] · Abdelkader Tadjer[5]**

Received: 7 November 2020 / Accepted: 10 May 2021 / Published online: 10 June 2021


**Abstract**
The first principle methods are employed to determine the electronic properties, half-metallic ferromagnetism and exchange splitting in $Ba_{1-x}Ti_xO$ compound based on titanium (Ti)-doped BaO at concentration $x=0.125$. The generalised gradient functional of Wu and Cohen is utilized to characterize the structural parameters of both BaO and $Ba_{0.875}Ti_{0.125}O$ materials, whereas the Tran-Blaha-modified Becke-Johnson potential is used to calculate the magnetic properties and electronic structures with perfect band gaps. The variations of lattice constants and bulk modulus of $Ba_{0.875}Ti_{0.125}O$ were investigated. In $Ba_{0.875}Ti_{0.125}O$, the ferromagnetic arrangement is mainly endorsed by the direct exchange splitting. The $Ba_{0.875}Ti_{0.125}O$ compound is true half-metallic ferromagnetic and 100% spin polarization with a half-metallic gap of 0.803 eV. Consequently, the $Ba_{0.875}Ti_{0.125}O$ can be considered as potential material for spintronics.

**Keywords** Electronic properties · Exchange splitting · Ferromagnetism · Spintronics

✉ Malika Hachemaoui
malika.hachemaoui@univ-saida.dz

✉ Bendouma Doumi
bendouma.doumi@univ-saida.dz

[1] Faculty of Sciences, Department of Physics, University of Saida Dr. Moulay Tahar, 20000 Saida, Algeria

[2] Instrumentation and Advanced Materials Laboratory, University Center of Nour Bachir El-Bayadh, 32000 El-Bayadh, Algeria

[3] University Center of Nour Bachir El-Bayadh, 32000 El-Bayadh, Algeria

[4] Department of Engineering Physics, Ankara University, 06100 Tandogan, Ankara, Turkey

[5] Modelling and Simulation in Materials Science Laboratory, Physics Department, Djillali Liabes University of Sidi Bel-Abbes, 22000 Sidi Bel-Abbes, Algeria

## 1 Introduction

Spintronics is an attractive field of research into spin-based physical phenomena and electronics, it is known as spin electronics because the spin of electron plus is used to improve the performance of spin-based electronic devices (Wolf et al. 2001; Liu et al. 2019). Recently, the diluted magnetic semiconductors (DMS) are realized from the rare earth and transition metal atoms doped semiconductors, they have been widely investigated as promising candidates for several spintronics applications due to their intermediate properties, which combine magnetic and semiconductor behaviours (Pan et al. 2008; Poornaprakash et al. 2020; Doumi et al. 2013). The half-metallic ferromagnets DMS have been considered an important class of materials for spintronics applications because their electronic structures reveal a semiconductor feature in one spin directions and a metallic character in the other spin channel (Hirohata et al. 2020; Korichi et al. 2020). However, spintronics utilizes both spin and charge of electron to generate new functionalities in spin-based devices. The advantages of spintronics devices with respect to the conventional electronics are the non-volatility, reduced energy consumption, high transistor density and fast data processing. (Kaminska et al. 2008; Goktas 2020; Khandy et al. 2019).

The alkaline-earth-metal binary oxides have been considered as potential materials for spintronics and optoelectronics applications (Kenmochi et al. 2004a, b; Albanese and Pacchioni 2017). The barium oxide (BaO) is one of the alkaline-earth-metal with wide band gap (Yang et al. 2016), it has several technological applications for example its use as a bumper layer on silicon in the epitaxial growth of perovskite oxides (Yang et al. 2016; McKee et al. 2001). The half-metallic ferromagnetic property was predicted in the new class of DMS based on C-doped MgO, SrO and BaO (Kenmochi et al. 2004a) and CaO doped with C and N atoms (Kenmochi et al. 2004b). Albanese and Pacchioni (2017) have investigated magnetic interaction of nitrogen N-doped BaO using first-principle approaches. The BaO is a potential candidate for spintronics according to first-principle study, revealing a half-metallic ferromagnetic behavior in the BaO under the effect of chromium (Cr) doping (Lakhdari et al. 2019).

In this work, we have studied the structural parameters, electronic properties, induced ferromagnetism, half-metallic behavior, exchange splitting and crystal field energy in the $Ba_{1-x}Ti_xO$ compound with concentration $x=0.125$ of titanium (Ti). The calculations were carried out by using the first-principle methods of full-potential linearized augmented plane-wave (FP-LAPW) approach (Singh and Nordstrom 2006) and density functional theory (DFT) (Hohenberg and Kohn 1964; Kohn and Sham 1965).

## 2 Method of calculations

The structural, magnetic properties and electronic structures of $Ba_{1-x}Ti_xO$ were determined by utilizing the first-principle concepts of the FP-LAPW approach and the DFT implemented in WIEN2k code (Blaha et al. 2001). The structural properties of $Ba_{1-x}Ti_xO$ at $x=0.125$ and BaO compound are determined by the use of the GGA-WC functional (Wu and Cohen 2006), whereas the Tran–Blaha-modified Becke–Johnson exchange potential (TB-mBJ) combined with the local density approximation (Tran and Blaha 2009; Koller et al. 2011) is employed to compute the magnetic moments,

exchange constants, exchange splitting, crystal field energy and electronic structures with perfect bands gaps of $Ba_{0.875}Ti_{0.125}O$.

In the interstitial sites of crystal, the wave functions have been extended to plane waves by means of a cut-off of $k_{max}\ R_{MT}=8.0$, where the $k_{max}$ corresponds to the largest $k$ vector in the plane wave and the $R_{MT}$ represents the mean radius of the sphere of muffin-tin. The charge density is Fourier extended up to $G_{max}=14$ (a.u.)$^{-1}$, where $G_{max}$ corresponds to the largest vector in the Fourier expansion, while the maximum value of the partial waves inside the atomic sphere is $l_{max}=10$. The core and valence states are separated by the cut-off of $-6$ Ry. The integration of the Brillouin zone is achieved by employing the Monkhorst–Pack technique (Monkhorst and Pack 1976), where the meshes of $(4\times4\times2)$ and $(4\times4\times4)$ are employed respectively for $Ba_{1-x}Ti_xO$ and BaO. The self-consistent is achieved by setting the convergence of the total energy at 0.1 mRy.

The calculations are based on the conventional BaO lattice with NaCl structure and space group of ($Fm\bar{3}m$) number 225, where the barium is located at the (0, 0, 0) position and oxygen at (0.5, 0.5, 0.5). We $Ba_8O_8$ supercell of 16 atoms is used to create the $Ba_7TiO_8$ supercell by the substitution of the Ba cationic site at the (0, 0, 0) position with the titanium (Ti) magnetic atom. Therefore, we get the $Ba_{0.875}Ti_{0.125}O$ ($x=0.125$) supercell with tetragonal structure and space group of *P*4/*mmm* number 123.

## 3 Results and discussions

### 3.1 Structural properties

We have determined the thermodynamic stability of $Ba_{0.785}Ti_{0.125}O$ compound in the ordered NaCl (B1) structure from the energy of formation, which is given by the following expression (Bai et al. 2011; Doumi et al. 2015a):

$$E_{form} = E_{total}(Ba_{8-z}Ti_zO_8) - \left(\frac{(8-z)\,E(Ba)}{16}\right) - \left(\frac{z\,E(Ti)}{16}\right) - \left(\frac{8\,E(O)}{16}\right)$$

where the $E_{total}(Ba_{8-z}Ti_zO_8)$ is the minimum total energy of $Ba_{8-z}Ti_zO_8$ per atom, while the minimum total energies per atom of bulks Ba, Ti and O correspond to the $E$(Ba), $E$(Ti) and $E$(O), respectively. In the case of the $Ba_{0.785}Ti_{0.125}O$ material, z equal to 1, which refers to the substituted Ti atom in the $Ba_{8-y}Ti_yO_8$ structure. The calculated formation energy of $-5.12$ eV is negative, which means that the $Ba_{0.785}Ti_{0.125}O$ compound is thermodynamically stable and it can be synthesized experimentally.

The lattice constants ($a$), bulk modules ($B$) and their pressure derivatives ($B'$) of BaO and $Ba_{0.785}Ti_{0.125}O$ compounds are calculated by the fit of the empirical Murnaghan's equation (Murnaghan 1944). The computed values of structural parameters are shown in Table 1 with other experimental values (Liu and Bassett 1972; Kaneko et al. 1982; PARK and Sivertsen 1977; Chang and Graham 1977) and theoretical results (Yang et al. 2016; Lakhdari et al. 2019; Nejatipour and Dadsetani 2015; Cinthia et al. 2015; Santana et al. 2016). We have noticed that there are changes in the values of lattice constant and bulk modulus of $Ba_{0.875}Ti_{0.125}O$ doping material compared to the BaO. This is due to the difference in the sizes of ionic radii of Ba and Ti elements. However, the lattice constant of $Ba_{0.785}Ti_{0.125}O$ decreases with respect to the BaO, leading to the increase of bulk modulus of $Ba_{0.785}Ti_{0.125}O$. Therefore, the $Ba_{0.785}Ti_{0.125}O$ becomes harder than that BaO. The behaviours of these two parameters of $Ba_{0.785}Ti_{0.125}O$ material were observed for CaO

**Table 1** Calculated lattice constants ($a$), bulk modules ($B$) and their pressure derivatives ($B'$), and standard deviations ($\sigma$) of BaO and $Ba_{0.875}Ti_{0.125}O$ with other theoretical and experimental data

| Compound | $a$ (Å) | $B$ (GPa) | $B'$ | $\sigma$(Å) | Method |
|---|---|---|---|---|---|
| This work | | | | | GGA-WC |
| BaO | 5.506 | 78.60 | 5.03 | 0.089 | |
| $Ba_{0.875}Ti_{0.125}O$ | 5.393 | 83.35 | 4.86 | 0.066 | |
| Other calculations | | | | | |
| BaO | 5.539[a]<br>5.525[b] | 75.6[c] | 5.67[d] | | Experimental |
| | 5.507[e] | 78.59[e] | 4.9[e] | | GGA-WC |
| | 5.594[f] | | | | GGA-PBE |
| | 5.58[g] | | | | GGA-PBE |
| | 5.604[h] | 75[h] | 4.1[h] | | GGA-PBE |
| | 5.478[i] | 82.36[i] | 4.21[i] | | LDA |

[a](Liu and Bassett 1972), [b](Kaneko et al. 1982), [c](PARK and Sivertsen 1977), [d](Chang and Graham 1977), [e](Lakhdari et al. 2019), [f](Yang et al. 2016), [g](Nejatipour and Dadsetani 2015), [h](Cinthia et al. 2015), [i](Santana et al. 2016)

doped with Ti (Korichi et al. 2020) and BaO doped with chromium (Cr) (Lakhdari et al. 2019). It should be noted that the $Ba_{0.785}Ti_{0.125}O$ material has not been studied theoretically and experimentally, so our calculations of structural properties of $Ba_{0.785}Ti_{0.125}O$ cannot be compared to other studies. Besides, the calculated standard deviations of 0.089 and 0.066 Å respectively for BaO and $Ba_{0.785}Ti_{0.125}O$ are very low, indicating that our results for the lattice parameters are very close to the average of the values of our calculations, other theoretical and experimental data.

Moreover, the results of $a$ and $B$ parameters of BaO are consistent to the experimental results (Kaneko et al. 1982; Liu and Bassett 1972; PARK and Sivertsen 1977) and theoretical calculations (Lakhdari et al. 2019) found by GGA-WC (Wu and Cohen 2006). Also, these parameters are better than the theoretical values (Yang et al. 2016; Lakhdari et al. 2019; Nejatipour and Dadsetani 2015; Cinthia et al. 2015; Santana et al. 2016) calculated with generalised gradient functional of Perdew-Burke-Ernzerhof (GGA-PBE) (Perdew et al. 1996) and the local density approach (LDA) (Perdew and Zunger 1981) with respect to the experimental values, meaning that the GGA-WC (Wu and Cohen 2006) provides good values for the structural properties due to its the performance for determining structural properties compared to other approximations (Wu and Cohen 2006; Doumi et al. 2015c; Sajjad et al. 2015; Bourega et al. 2019). The performance of the GGA-WC approximation for computing the structural parameters results from the fourth-order gradient expansion of exchange and correlation of its gradient functional (Wu and Cohen 2006; Doumi et al. 2015b, 2020).

### 3.2 Electronic structures

Firstly, we have determined the electronic properties of the BaO and $Ba_{0.875}Ti_{0.125}O$ compounds, and then we have studied the effect of the titanium (Ti) magnetic atoms on the half-metallic property and the origin of ferromagnetic arrangement in $Ba_{0.875}Ti_{0.125}O$. Figures 1 and 2 show the band structures of BaO and $Ba_{0.875}Ti_{0.125}O$, respectively. The projected total and partial densities of states (DOS) of $Ba_{0.875}Ti_{0.125}O$ are displayed by the Figs. 3 and 4 respectively. The Fig. 1 shows that there is a band

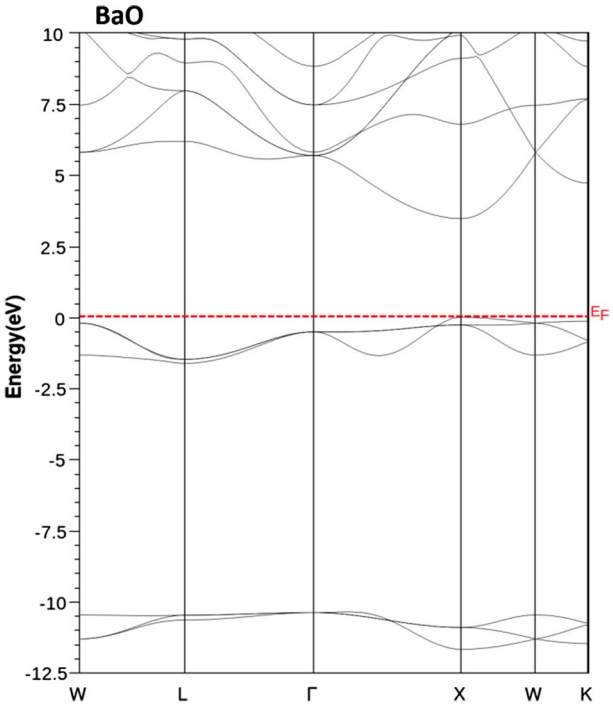


**Fig. 1** Band structures for BaO

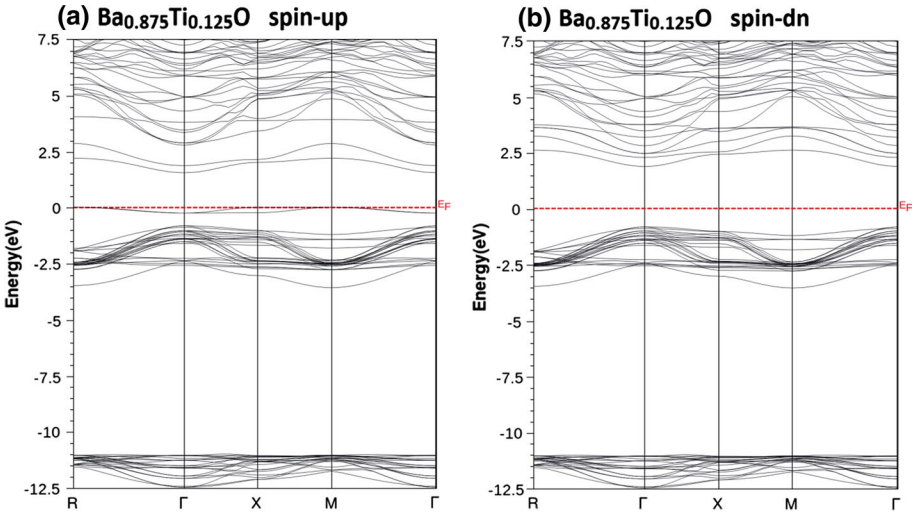


**Fig. 2** Spin-polarized band structures for $Ba_{0.875}Ti_{0.125}S$, **a** Majority spins (*up*) and **b** Minority spins (*dn*)

gap around Fermi level because all electron states are bound to the valance band, which means that BaO bulk has semiconductor nature. The maximum of the valence band and the minimum of the conduction band occur at the same X high symmetry point, revealing direct gap ($E^{XX}$) for BaO. For the $Ba_{0.875}Ti_{0.125}O$ doping system, the band structures

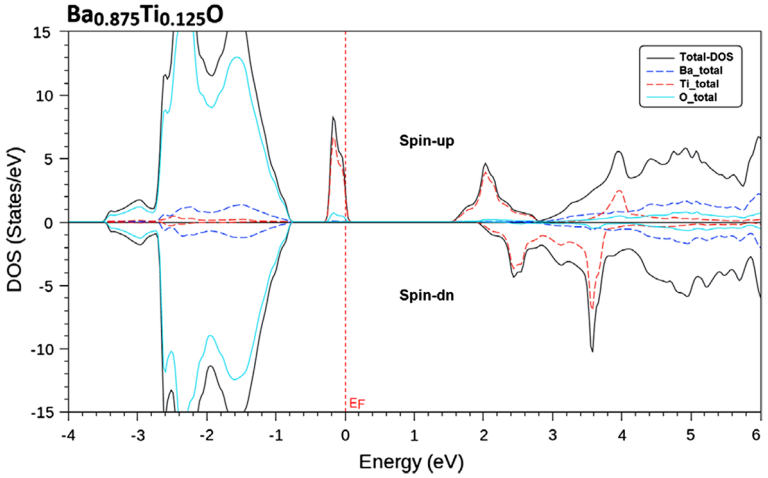


**Fig. 3** Spin-polarized total densities of states (DOS) of Ba, O and Ti atoms and total-DOS for $Ba_{0.875}Ti_{0.125}O$

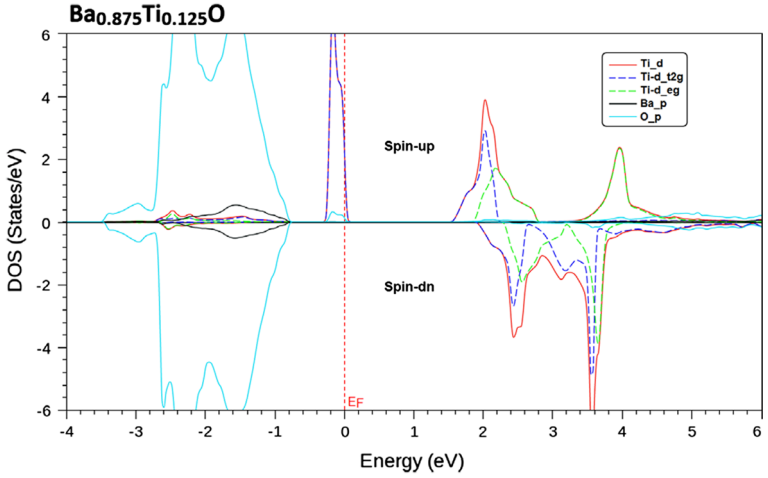


**Fig. 4** Spin-polarized partial densities of Ti_d, Ti-d_$t_{2g}$, Ti-d_$e_g$, Ba_p and O_p states for $Ba_{0.875}Ti_{0.125}O$

show different behavior compared to the BaO bulk due to the magnetic character of injected Ti atoms. The minority-spin bands keep the semiconductor feature, but the majority-spin bands become metallic as shown in Fig. 2.

From Fig. 3, the metallic character of majority spins results from the localized magnetic spins of 3d (Ti) states around $E_F$, while the minority spins have unoccupied 3d (Ti) states sited at the lower part of the conduction band. Consequently, the $Ba_{1-x}Ti_xO$ reflects a perfect half-metallic ferromagnetic behavior. The direct band gap of minority-spin bands located at the X high symmetry point is called the half-metallic ferromagnetic (HMF) gap ($G_{HMF}$), whereas the minimum energy located between the Fermi energy ($E_F$) (0 eV) and the maximum of valence band corresponds to the half-metallic

(HM) gap ($G_{HM}$). In the case of the minority spins of $Ba_{0.875}Ti_{0.125}O$ material, the HM gap describes the absolute energy of maximum of valence band with respect to the $E_F$. The Table 2 summarizes the calculated HM ferromagnetic band gap and HM band gap of minority spins of $Ba_{0.875}Ti_{0.125}O$ and direct band gap ($E^{XX}$) of BaO, with other theoretical (Yang et al. 2016; Lakhdari et al. 2019; Nejatipour and Dadsetani 2015; McLeod et al. 2010; Teli and Sirajuddeen 2019) and experimental (Zollweg 1958; Saum and Hensley 1959; Kaneko and Koda 1988) values. The $Ba_{0.875}Ti_{0.125}O$ material has a ferromagnetic half-metallic gap ($G_{HMF}$) and a half-metallic gap ($G_{HM}$) of 2.701and 0.803 eV, respectively. The $Ba_{0.875}Ti_{0.125}O$ has direct half-metallic ferromagnetic gap ($G_{HMF}$) positioned at Γ point, although the half-metallic gap ($G_{HM}$) arises between the Fermi level and maximum of valence bands. The direct wide gap of 3.5 eV of BaO calculated with the TB-mBJ is more improved with respect to the theoretical values (Yang et al. 2016; Lakhdari et al. 2019; Nejatipour and Dadsetani 2015; McLeod et al. 2010; Teli and Sirajuddeen 2019) found by the GGA-WC (Wu and Cohen 2006), GGA-PBE (Perdew et al. 1996) and LDA (Perdew and Zunger 1981). The better gap of BaO is due to the performance of TB-mBJ for predicting values of band gaps of semiconductors and insulators (Koller et al. 2011; Bhattacharjee and Chattopadhyaya 2017; Chattopadhyaya and Bhattacharjee 2017).

The $Ba_{0.875}Ti_{0.125}O$ material is doped by the titanium (Ti) transition atom, which is characterized by the 3d electronic levels localized in the gap around $E_F$ of majority spins as seen in Fig. 4. The main part of the total-DOS of majority spins at $E_F$ is originated from the contributions of the Ba and Ti atoms. The metallic nature of majority spins results from the p-d hybridization of electronic states of 3d of titanium and p of oxygen as shown in Fig. 4. In addition, the 3d levels of titanium are splitted into $t_{2g}$ partially occupied states and $e_g$ empty states due to the octahedral crystal field environment originated form neighbouring oxygen ions. From Fig. 3, we can see clearly that the total-DOS is metallic for the majority spins but a semiconductor character occurs around $E_F$ for the minority spins. Consequently, the $Ba_{0.875}Ti_{0.125}O$ material has half-metallic ferromagnetic feature and it can be considered as a potential compound for spintronics applications.

**Table 2** Computed direct gap $E^{XX}$ of BaO, half-metallic ferromagnetic gap ($G_{HMF}$) and half-metallic gap ($G_{HM}$) of minority-spin bands of $Ba_{0.875}Ti_{0.125}O$ with other theoretical and experimental data

| Compound | $G_{HMF}$ (eV) | $G_{HM}$ (eV) | $E^{XX}$ (eV) | Method |
|---|---|---|---|---|
| This work | | | | TB-mBJ |
| BaO | | | 3.476 | |
| $Ba_{0.875}Ti_{0.125}O$ | 2.701 | 0.803 | | |
| *Other calculations* | | | | |
| BaO | | | 1.884[a] | GGA-WC |
| | | | 2.08[b] | GGA-PBE |
| | | | 2.32[c] | GGA-PBE |
| | | | 2.0 [d] | GGA-PBE |
| | | | 2.14[e] | GGA-PBE |
| | | | 3.88[f] | Experimental |
| | | | 4.1 [g] | |
| | | | 3.985 [h] | |

[a](Lakhdari et al. 2019), [b](Yang et al. 2016), [c](Nejatipour and Dadsetani 2015), [d](McLeod et al. 2010), [e](Teli and Sirajuddeen 2019), [f](Zollweg 1958), [g](Saum and Hensley 1959), [h](Kaneko and Koda 1988)

### 3.3 Magnetic properties

#### 3.3.1 Magnetic moments

The origin of magnetism in the $Ba_{0.875}Ti_{0.125}O$ compound is due to the localization of the partially occupied 3d states of Ti of the majority spins around $E_F$. The Fig. 4 of majority spins shows that the $e_g$ states are unoccupied, while the $t_{2g}$ states are two-thirds filled. Thus, the $t_{2g}$ levels are partially occupied by two electrons, which induce a total magnetic moment of 2 $\mu_B$. The results of computed total and local magnetic moments of $Ba_{0.875}Ti_{0.125}O$ compound are given in Table 3. We have found that the magnetic moment of Ti of 1.778 $\mu_B$ is reduced below the value of 2 $\mu_B$ and little moments are induced at the Ba, O sites. The negative moment of O atom indicates that the interaction between the (Ba, Ti) and O magnetic spins is anti-ferromagnetic. The Ba and Ti positive moments generate ferromagnetic interaction.

#### 3.3.2 Exchange couplings

The exchange interactions between the conduction or the valence bands and electronic states of 3d states of titanium are explained by the $N_0\alpha$ and $N_0\beta$ exchange parameters. The $N_0\alpha$ describes the exchange coupling between the s-type of conduction bands and 3d levels of titanium, whereas the $N_0\beta$ determines the exchange coupling between the p-type of valence bands and 3d levels of titanium. The $N_0\alpha$ and $N_0\beta$ constants are computed by using the mean-field theory, given by the following relations (Sanvito et al. 2001; Raebiger et al. 2004):

$$N_0\alpha = \frac{\Delta E_c}{x\langle s\rangle} \tag{1}$$

$$N_0\beta = \frac{\Delta E_v}{x\langle s\rangle} \tag{2}$$

where the $\Delta E_c = E_c^{\downarrow} - E_c^{\uparrow}$ and $\Delta E_v = E_v^{\downarrow} - E_v^{\uparrow}$ correspond respectively to the conduction and valence band-edge spin-splittings at Γ high symmetry point of $Ba_{0.875}Ti_{0.125}O$. The $\langle s\rangle$ represents the half total magnetic moment per Ti and $x = 0.125$ is the concentration of Ti atom (Sanvito et al. 2001). Table 4 summarizes the calculated $N_0\alpha$ and $N_0\beta$ exchange parameters of $Ba_{0.875}Ti_{0.125}O$ compound. Its shows that the $N_0\alpha$ is positive and $N_0\beta$ is negative, revealing ferromagnetic and anti-ferromagnetic exchange couplings respectively between conduction bands and d (Ti) orbitals and between the valence bands and d electronic levels of titanium.

**Table 3** Calculated total and partial magnetic moments and in the interstitial sites of $Ba_{0.875}Ti_{0.125}O$

| Compound | Total ($\mu_B$) | Ti ($\mu_B$) | Ba ($\mu_B$) | O ($\mu_B$) | Interstitial ($\mu_B$) |
|---|---|---|---|---|---|
| $Ba_{0.875}Ti_{0.125}O$ | 2 | 1.778 | 0.002 | −0.012 | 0.234 |

**Table 4** Computed sp-d exchange constants $N_0\alpha$ and $N_0\beta$, crystal field energy $\Delta E_{CF}$ and direct exchange splitting $\Delta_x(d)$ of $Ba_{0.875}Ti_{0.125}O$

| Compound | $N_0\alpha$ | $N_0\beta$ | $\Delta_x(d)$(eV) | $\Delta E_{CF}$(eV) |
|---|---|---|---|---|
| $Ba_{0.875}Ti_{0.125}O$ | 1.344 | −2.273 | 3.755 | 4.136 |

### 3.3.3 Exchange splittings

The magnitude of ferromagnetism is measured by the use of two factors such as direct exchange and crystal field splittings. The energy that separate the d (Ti) empty levels ($d\downarrow$) of minority spins and the d (Ti) partially filled levels ($d\uparrow$) of majority spins corresponds to the direct exchange splitting ($\Delta_x(d) = d\downarrow - d\uparrow$). The crystal field splitting ($\Delta E_{CF} = E_{eg} - E_{t2g}$) is described by the splitting between the $E_{eg}$ and $E_{t2g}$ energies respectively for $e_g$ of $t_{2g}$ states. It has been reported that the ferromagnetic state in $Ca_{0.875}Ti_{0.125}O$ compound is mainly predominated by the crystal field energy (Korichi et al. 2020). For our material, the Fig. 4 depicted that the $e_g$ peaks are located at high levels with respect to the unoccupied ($d\downarrow$) minority-spin states, but the peaks of ($d\uparrow$) and $t_{2g}$ partially occupied states of majority spins occur at the same level with respect to $E_F$. Therefore, the ($\Delta E_{CF}$) crystal field splitting is mainly contributed over the $\Delta_x(d)$ splitting. This result is revealed by the smaller value of 3.755 eV of the $\Delta_x(d)$ splitting compared to the ($\Delta E_{CF}$) energy of 4.136 eV as seen in Table 4. This kind of process reveals that the crystal field contribution endorses mostly the ferromagnetic state compared to the indirect exchange splitting.

## 4 Conclusion

We have used the concepts of DFT and FP-LAPW methods to determine the electronic properties, structural parameters, half-metallic ferromagnetic feature, exchange constants, crystal field energy and exchange splittings in the $Ba_{1-x}Ti_xO$ doped with titanium (Ti) impurity at the concentration $x = 0.125$ such as $Ba_{0.875}Ti_{0.125}O$ compound. The calculated structural parameters of BaO bulk agree with theoretical and experimental results owing to the accurate GGA-WC functional for predicting structural parameters. The lattice parameter of $Ba_{0.875}Ti_{0.125}O$ decreases, leading to the variation of the bulk modulus towards higher value compared to the BaO. These changes result from the size distinction of ionic radii of the Ba and Ti elements. The calculations of TB-mBJ potential revealed that the BaO has a semiconductor character with wide direct band gap, whereas the $Ba_{0.875}Ti_{0.125}O$ doping compound has a integral total magnetic moment with spin polarization of 100% and a half-metallic ferromagnetic behavior. The crystal field contribution endorses mainly the ferromagnetic state in $Ba_{0.875}Ti_{0.125}O$. Consequently, the $Ba_{0.875}Ti_{0.125}O$ is an accurate half-metallic ferromagnetic and it can be considered as a promising material for possible applications in semiconductors spintronics.

**Acknowledgements** There are no acknowledgments for our manuscript.

**Authors contributions** All authors contributed to the study conception and design. Material preparation, data collection and analysis were performed by all authors. The first draft of the manuscript was written

by author: MH and all authors commented on previous versions of the manuscript. All authors read and approved the final manuscript.

**Funding** There is no funding statement for our manuscript.

**Data availability** The authors declare that all data and material are included and available in the manuscript.

**Declarations**

**Conflict of interest** The authors declare that they have no conflict of interest.

**Human and animal rights** The authors declare that the manuscript does not contain Research involving Human Participants and/or Animals.

**Informed consent** There is no informed consent to declare for our manuscript.

## References

Albanese, E., Pacchioni, G.: Ferromagnetism in nitrogen-doped BaO: a self-interaction corrected DFT study. Phys. Chem. Chem. Phys. **19**(4), 3279–3286 (2017)

Bai, J., Raulot, J.-M., Zhang, Y., Esling, C., Zhao, X., Zuo, L.: The effects of alloying element Co on Ni–Mn–Ga ferromagnetic shape memory alloys from first-principles calculations. Appl. Phys. Lett. **98**(16), 164103 (2011)

Bhattacharjee, R., Chattopadhyaya, S.: Effects of barium (Ba) doping on structural, electronic and optical properties of binary strontium chalcogenide semiconductor compounds—a theoretical investigation using DFT based FP-LAPW approach. Mater. Chem. Phys. **199**, 295–312 (2017)

Blaha, P., Schwarz, K., Madsen, G.K.H., Kvasnicka, D., Luitz, J.: WIEN2K: an augmented plane wave and local orbitals program for calculating crystal properties. In: Vienna, K. (ed.) University of Technology, Schwarz, Austria (2001)

Bourega, A., Doumi, B., Mokaddem, A., Sayede, A., Tadjer, A.: Electronic structures and magnetic performance related to spintronics of $Sr_{0.875}Ti_{0.125}S$. Opt. Quant. Electron **51**(12), 385 (2019)

Chang, Z., Graham, E.: Elastic properties of oxides in the NaCl-structure. J. Phys. Chem. Solids **38**(12), 1355–1362 (1977)

Chattopadhyaya, S., Bhattacharjee, R.: Theoretical study of structural, electronic and optical properties of $Ba_xPb_{1-x}S$, $Ba_xPb_{1-x}Se$ and $Ba_xPb_{1-x}Te$ ternary alloys using FP-LAPW approach. J. Alloy. Compd. **694**, 1348–1364 (2017)

Cinthia, A.J., Priyanga, G.S., Rajeswarapalanichamy, R., Iyakutti, K.: Structural, electronic and mechanical properties of alkaline earth metal oxides MO (M= Be, Mg, Ca, Sr, Ba). J. Phys. Chem. Solids **79**, 23–42 (2015)

Doumi, B., Tadjer, A., Dahmane, F., Mesri, D., Aourag, H.: Investigations of structural, electronic, and half-metallic ferromagnetic properties in $(Al, Ga, In)_{1-x}$ $M_xN$ (M= Fe, Mn) diluted magnetic semiconductors. J. Supercond. Novel. Magn. **26**(3), 515–525 (2013)

Doumi, B., Mokaddem, A., Ishak-Boushaki, M., Bensaid, D.: First-principle investigation of magnetic and electronic properties of vanadium-and chromium-doped cubic aluminum phosphide. Sci. Semicond. Process. **32**, 166–171 (2015a)

Doumi, B., Mokaddem, A., Sayede, A., Dahmane, F., Mogulkoc, Y., Tadjer, A.: First-principles investigations on ferromagnetic behaviour of $Be_{1-x}V_xZ$ (Z= S, Se and Te)(x= 0.25). Superlattice. Microstruct. **88**, 139–149 (2015b)

Doumi, B., Mokaddem, A., Temimi, L., Beldjoudi, N., Elkeurti, M., Dahmane, F., Sayede, A., Tadjer, A., Ishak-Boushaki, M.: First-principle investigation of half-metallic ferromagnetism in octahedrally bonded Cr-doped rock-salt SrS, SrSe, and SrTe. Eur. Phys. J. B **88**(4), 93 (2015c)

Doumi, B., Mokaddem, A., Tadjer, A., Sayede, A.: Recent insights into electronic performance, magnetism and exchange splittings in the Cr-substituted CaO. Front. Chem. **8**, 526 (2020)

Goktas, A.: Role of simultaneous substitution of Cu2+ and Mn2+ in ZnS thin films: defects-induced enhanced room temperature ferromagnetism and photoluminescence. Phys. e. **117**, 113828 (2020)

Hirohata, A., Yamada, K., Nakatani, Y., Prejbeanu, L., Diény, B., Pirro, P., Hillebrands, B.: Review on spintronics: principles and device applications. J. Magn. Magn. Mater. **509**, 166711 (2020)

Hohenberg, P., Kohn, W.: Inhomogeneous electron gas. Phys. Rev. **136**(3B), B864-871 (1964)
Kaminska, M., Twardowski, A., Wasik, D.: Mn and other magnetic impurities in GaN and other III–V semiconductors–perspective for spintronic applications. J. Mater. Sci. Mater. El **19**(8–9), 828–834 (2008)
Kaneko, Y., Koda, T.: New developments in IIa–VIb (alkaline-earth chalcogenide) binary semiconductors. J. Cryst. Growth **86**(1–4), 72–78 (1988)
Kaneko, Y., Morimoto, K., Koda, T.: Optical properties of alkaline-earth chalcogenides. I. Single crystal growth and infrared reflection spectra due to optical phonons. J. Phys. Soc. Jpn. **51**(7), 2247–2254 (1982)
Kenmochi, K., Ann Dinh, V., Sato, K., Yanase, A., Katayama-Yoshida, H.: Materials design of transparent and half-metallic ferromagnets of MgO, SrO and BaO without magnetic elements. J. Phys. Soc. Jpn. **73**(11), 2952–2954 (2004a)
Kenmochi, K., Seike, M., Sato, K., Yanase, A., Katayama-Yoshida, H.: New class of diluted ferromagnetic semiconductors based on CaO without transition metal elements. Jpn. J. Appl. Phys. **43**(7A), L934–L936 (2004b)
Khandy, S.A., Islam, I., Gupta, D.C., Laref, A.: Full Heusler alloys ($Co_2TaSi$ and $Co_2TaGe$) as potential spintronic materials with tunable band profiles. J. Solid. State. Chem. **270**, 173–179 (2019)
Kohn, W., Sham, L.J.: Self-consistent equations including exchange and correlation effects. Phys. Rev. **140**(4A), A1133–A1138 (1965)
Koller, D., Tran, F., Blaha, P.: Merits and limits of the modified Becke–Johnson exchange potential. Phys. Rev. B **83**(19), 195134 (2011)
Korichi, K., Doumi, B., Mokaddem, A., Sayede, A., Tadjer, A.: Ferromagnetism, half-metallicity and spin-polarised electronic structures characterisation insights in $Ca_{1-x}Ti_xO$. Philos. Mag. **100**(9), 1172–1190 (2020)
Lakhdari, H., Doumi, B., Mokaddem, A., Sayede, A., Araújo, J.P., Tadjer, A., Elkeurti, M.: Investigation of the substituting effect of chromium on the electronic structures and the half-metallic ferromagnetic properties of BaO. J. Supercond. Novel. Magn. **32**(6), 1781–1790 (2019)
Liu, L.G., Bassett, W.A.: Effect of pressure on the crystal structure and the lattice parameters of BaO. J. Geophys. Res. **77**(26), 4934–4937 (1972)
Liu, W., Wong, P.K.J., Xu, Y.: Hybrid spintronic materials: growth, structure and properties. Prog. Mater. Sci. **99**, 27–105 (2019)
McKee, R., Walker, F., Chisholm, M.: Physical structure and inversion charge at a semiconductor interface with a crystalline oxide. Science **293**(5529), 468–471 (2001)
McLeod, J., Wilks, R., Skorikov, N., Finkelstein, L., Abu-Samak, M., Kurmaev, E., Moewes, A.: Band gaps and electronic structure of alkaline-earth and post-transition-metal oxides. Phys. Rev. B **81**(24), 245123 (2010)
Monkhorst, H.J., Pack, J.D.: Special points for Brillouin-zone integrations. Phys. Rev. B **13**(12), 5188–5192 (1976)
Murnaghan, F.: The compressibility of media under extreme pressures. Proc. Natl. Acad. Sci. U.s.a. **30**(9), 244–247 (1944)
Nejatipour, H., Dadsetani, M.: Excitonic effects in the optical properties of alkaline earth chalcogenides from first-principles calculations. Phys. Scr. **90**(8), 085802 (2015)
Pan, F., Song, C., Liu, X., Yang, Y., Zeng, F.: Ferromagnetism and possible application in spintronics of transition-metal-doped ZnO films. Mat. Sci. Eng. R **62**(1), 1–35 (2008)
PARK, K.O., Sivertsen, J.: Temperature dependence of the bulk modulus of BaO single crystals. J. Am. Ceram. Soc. **60**(11–12), 537–538 (1977)
Perdew, J.P., Zunger, A.: Self-interaction correction to density-functional approximations for many-electron systems. Phys. Rev. B **23**(10), 5048–5079 (1981)
Perdew, J.P., Burke, K., Ernzerhof, M.: Generalized gradient approximation made simple. Phys. Rev. Lett. **77**(18), 3865–3868 (1996)
Poornaprakash, B., Chalapathi, U., Kumar, M., Rajitha, B., Reddy, B.P., Vattikuti, S.P., Park, S.-H.: Tailoring the optical, magnetic, and photocatalytic properties of ZnS quantum dots by rare-earth ion doping. Chem. Phys. Lett. 137609 (2020)
Raebiger, H., Ayuela, A., Nieminen, R.: Intrinsic hole localization mechanism in magnetic semiconductors. J. Phys. Condens. Matter. **16**(41), L457–L462 (2004)
Sajjad, M., Manzoor, S., Zhang, H., Noor, N., Alay-e-Abbas, S., Shaukat, A., Khenata, R.: The half-metallic ferromagnetism character in $Be_{1-x}V_xY$ (Y= Se and Te) alloys: an ab-initio study. J. Magn. Magn. Mater. **379**, 63–73 (2015)
Santana, J.A., Krogel, J.T., Kent, P.R., Reboredo, F.A.: Cohesive energy and structural parameters of binary oxides of groups IIA and IIIB from diffusion quantum Monte Carlo. J. Chem. Phys. **144**(17), 174707 (2016)

Sanvito, S., Ordejón, P., Hill, N.A.: First-principles study of the origin and nature of ferromagnetism in $Ga_{1-x}Mn_xAs$. Phys. Rev. B **63**(16), 165206 (2001)
Saum, G.A., Hensley, E.B.: Fundamental optical absorption in the IIA-VIB compounds. Phys. Rev. **113**(4), 1019–1022 (1959)
Singh, D.J., Nordstrom, L.: Planewaves, pseudopotentials, and the LAPW method. Springer (2006)
Teli, N.A., Sirajuddeen, M.M.S.: First-principles calculations of the electronic, magnetic and optical properties of rhenium-doped alkaline earth oxides. Phys. Scr. **95**(2), 025801 (2019)
Tran, F., Blaha, P.: Accurate band gaps of semiconductors and insulators with a semilocal exchange-correlation potential. Phys. Rev. Lett. **102**(22), 226401 (2009)
Wolf, S., Awschalom, D., Buhrman, R., Daughton, J., von Molnár, V.S., Roukes, M., Chtchelkanova, A.Y., Treger, D.: Spintronics: a spin-based electronics vision for the future. Science **294**(5546), 1488–1495 (2001)
Wu, Z., Cohen, R.E.: More accurate generalized gradient approximation for solids. Phys. Rev. B **73**(23), 235116 (2006)
Yang, X., Wang, Y., Yan, H., Chen, Y.: Effects of epitaxial strains on spontaneous polarizations and band gaps of alkaline-earth-metal oxides MO (M = Mg, Ca, Sr, Ba). Comput. Mater. Sci. **121**, 61–66 (2016)
Zollweg, R.: Optical absorption and photoemission of barium and strontium oxides, sulfides, selenides, and tellurides. Phys. Rev. **111**(1), 113–119 (1958)